Transient Raman Scattering Study of the Initial Semiquinone Radical Kinetics following Photolysis of Aqueous Benzoquinone and Hydroquinone

S. M. Beck and L. E. Brus*

Contribution from Bell Laboratories, Murray Hill, New Jersey 07974.
Received November 16, 1981

Abstract: The photochemistry and photophysics of the title compounds in water and in mixed water–methanol solvents have been observed via transient spontaneous Raman spectroscopy. Strong resonance Raman signals are observed from the lowest benzoquinone triplet and from both the semiquinone radical and anion. The principal Raman transitions are assigned. Photooxidation of water, hydrogen atom extraction from methanol, and semiquinone acid–base equilibrium kinetics are observed. Possible biological kinetic experiments with naturally occurring quinones are discussed.

The importance of quinones as electron carriers in electrochemical and biological processes, including photosynthesis, provides strong incentive for an understanding of quinone photoredox kinetics. In a recent paper (hereafter labeled part 1), we reported that aqueous *p*-benzoquinone photooxidizes water via two-photon and (apparently) weak one-photon processes.[1] Using the technique of transient spontaneous Raman spectroscopy, we identified and followed the kinetics of the *p*-benzoquinone triplet [$Q(T_1)$], semiquinone radical anion [$Q^{-}\cdot$], and neutral radical [$QH\cdot$]. The transient absorption spectra of these species substantially overlap. We now describe in greater detail these observations and the reactions of $Q(T_1)$ with CH_3OH. We also include observation of $Q^{-}\cdot$ and $QH\cdot$ via photolysis of aqueous hydroquinone [QH_2].

Previous flash-photolysis studies have principally concentrated on tetramethyl-*p*-benzoquinone (duroquinone), presumably because the transients are spectrally separated. In this system, the triplet, formed in high quantum yield, does not react with water but can abstract H atoms or electrons from alcohols and hydrocarbons. Different workers appear to disagree on the primary steps.[2-4] In our Raman experiments, we detect the products $Q^{-}\cdot$ and $QH\cdot$ before an acid–base equilibrium is established. In favorable cases, we are able to estimate the initial $[Q^{-}\cdot]/[QH\cdot]$ ratio.

We employ transient spontaneous Raman spectroscopy in an attempt to understand chemical kinetics, not to generate radical spectra per se. The high sensitivity of Raman spectra to structure, and hence to subtle reaction and to isotopic substitution, normally produces a clearer kinetic picture than does transient absorption spectroscopy. The principal drawback of transient Raman studies is low detection sensitivity, reflecting the small absolute magnitude of the Raman cross section. We have previously discussed methods for increasing detection sensitivity and hence the range of chemical problems that can be usefully undertaken.[5]

Experimental Section

The Raman technology of pulsed excitation with multichannel optical detection has been pioneered by Bridoux and Delhaye.[6] Our techniques and apparatus have been recently described in detail.[5a] Briefly, there are two independent Nd:YAG lasers. The pump laser is frequency quadrupled to 266 nm; the probe laser is tripled to 355 nm and then Raman shifted to either 416 nm or 448 nm. The pump and probe pulses are spatially superimposed in a flowing liquid sample. Transient species created by the pump pulse have their Raman spectra generated by the probe pulse after a time delay Δt. The time resolution is limited to about 10 ns by the widths of the two pulses. The entire Raman spectrum is detected for each pulse pair with a grated, intensified Reticon multichannel detector. Extensive signal averaging improves the detection sensitivity.

Q and QH_2 were sublimed immediately prior to use. Solutions prepared with deionized water were shielded from room light and used within a few minutes of preparation. The pH was adjusted with HCl, and with DCl in D_2O solvent. High-pH solutions were not studied as both species are unstable in such solutions. Solutions were not deaerated.

Table I. Major 416-nm Resonance Raman Transitions (cm^{-1}) of the Indicated Species[a]

S_0	T_1	$Q^{-}\cdot$	$QH\cdot$	$QD\cdot$
			2094 (2)	2094 (2)
	1990 (2)		1984 (1)	1984 (2)
1671 (10)	1552 (10)	1622 (10)	1619 (10)	1615 (10)
	1497 (1)	1438 (2)	1515 (6)	1515 (7)
1163 (5)	1163 (4)	1163 (4)	1163 (3)	1163 (3)
		970 (0.5)	976 (0.5)	

[a] Numbers in parentheses are relative intensities.

Results

Acid–Base Equilibrium following QH_2 Photolysis. In paper 1 we described how the resonance Raman spectra of $Q(T_1)$, $Q^{-}\cdot$, and $QH\cdot$ can be distinguished and identified following excitation of aqueous Q. The $Q^{-}\cdot$ spectrum has also been recently observed via pulsed radiolysis.[7] In Figure 1, we report the 266-nm photolysis of QH_2. Trace a shows the 416-nm Raman spectrum (700–2500 cm^{-1}) observed at $\Delta t = 30$ ns after 266-nm photolysis of QH_2 at pH 6.7. This spectrum shows several sharp peaks on top of a continuum possessing a broad maximum near 1640 cm^{-1}. The continuum and 1640-cm^{-1} maximum are the Raman spectrum of water. The sharp peaks all belong to $QH\cdot$; the frequencies and relative intensities appear in Table I. The $QH\cdot$ signal is strong due to a moderate resonance Raman effect ($\epsilon_{416} \simeq 5000$ M^{-1} cm^{-1}[8]). The contribution of unphotolyzed QH_2 to this spectrum is orders of magnitude weaker; QH_2 is transparent at 416 nm and exhibits only ordinary Raman scattering. The absence of $Q^{-}\cdot$, which does show a 416-nm resonance Raman effect, implies that the initial yield of $Q^{-}\cdot$ is negligible.

The initial photolysis produces only $QH\cdot$ at our present experimental sensitivity. The reported pK_a of $QH\cdot$ is 4.1, however, so that when acid–base equilibrium is established at pH 6.7, the population must be entirely $Q^{-}\cdot$.[8] In agreement with this expectation, we observe the spectrum to evolve as Δt increases. This evolution is subtle as the spectrum of $Q^{-}\cdot$ has several peaks es-

(1) Beck, S. M.; Brus, L. E. *J. Am. Chem. Soc.* **1982**, *104*, 1103–1104.
(2) Kemp, D. R.; Porter, G. *Proc. R. Soc. London, Ser. A*, **1971**, *A326*, 117–130.
(3) Amouyal, E.; Bensasson, R. *J. Chem. Soc., Faraday Trans. 1*, **1976**, *72*, 1274–1287.
(4) Scheerer, R.; Grätzel, M. *J. Am. Chem. Soc.* **1977**, *99*, 865–871.
(5) (a) Beck, S. M.; Brus, L. E. *J. Chem. Phys.* **1981**, *75*, 4934–4940. (b) Beck, S. M.; Brus, L. E. *J. Chem. Phys.* **1981**, *75*, 1031–1033.
(6) Bridoux, M.; Delhaye, M. *Adv. Infrared Raman Spectrosc.* **1976**, *2*, 140–153.
(7) Tripathi, G. N. R. *J. Chem. Phys.* **1981**, *74*, 6044–6049.
(8) Patel, K. B.; Willson, R. L. *J. Chem. Soc., Faraday Trans. 1* **1973**, *69*, 814–825.

0002-7863/82/1504-4789$01.25/0

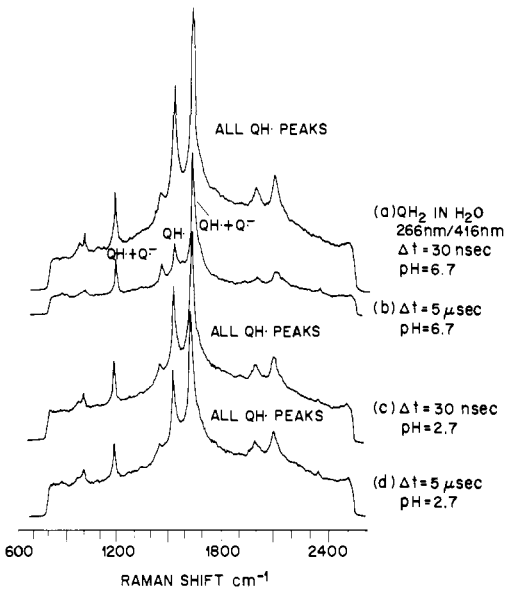

Figure 1. The 416-nm Raman spectra of aqueous hydroquinone (10^{-2} M) following 266-nm excitation at the indicated delays Δt and pH: 266-nm pulse energy $\simeq$ 10 mJ; 416-nm energy $\simeq$1 mJ. These spectra are an average of 600 pulse pairs at 10 Hz. QH· is the neutral semiquinone radical, and Q^-· is the semiquinone radical anion.

sentially in common with those of QH·. An identifying characteristic of QH· is a strong peak at 1515 cm^{-1} that is absent in Q^-·; both species have strong, partially overlapping peaks near 1620 cm^{-1}. Conversion of QH· to Q^-· would produce a decrease at 1515 cm^{-1} with respect to the composite 1620-cm^{-1} line. Trace b shows the observed spectrum $\Delta t = 5$ μs; the decreased 1515- to 1620-cm^{-1} ratio shows a significant conversion of QH· to Q^-· on this time scale. At pH 6.7, this is an apparent unimolecular dissociation QH· $\rightarrow$ Q^-· + H^+ not catalyzed by either $[H^+]$ or $[OH^-]$. An $\sim 10^{-6}$-s time scale is consistent for this dissociation with pK_a = 4.1 if the reverse Q^-· protonation process occurs at a diffusion-controlled rate of $\sim 10^{10}$ M^{-1} s^{-1}.

Traces c and d show no apparent evolution of the QH· spectrum at pH 2.7, in agreement with the reported pK_a. At both pH values there is an overall decrease in the transient Raman intensity with Δt, indicating some loss via reaction is occurring on this time scale.

Both radical species show $\epsilon_{416} \simeq 5000$ M^{-1} cm^{-1},[8] and we tentatively assume that their 416-nm resonance Raman cross sections are about equal. Quoted relative proportions between QH· and Q^-· refer to fitting of the resonance Raman spectra. These proportions are not concentration ratios unless the Raman cross sections are the same for both species. While the absorption cross sections are approximately equal, it is not necessarily true that the Raman cross sections are also equal.[9] Nevertheless, one might argue from the fact that the chromophores are essentially the same in QH· and Q^-· that the Raman cross sections will be similar.

At 448 nm, the Q^-· absorption is a factor of 10 (or more) stronger than that of QH·.[8] Thus, Q^-· should be relatively enhanced in 448-nm Raman spectra. Trace a of Figure 2 is the same as that of Figure 1a, with the exception of a 448-nm probe pulse. Both Q^-· and QH· contribute approximately equally to Figure 2a, in constrast to Figure 1a. Without knowing the relative 448-nm Raman cross sections, we cannot estimate the ratio of concentrations at Δt = 50 ns. The Q^-· signal increases approximately linearly with time for $\Delta t \leq 100$ ns, indicating that the Q^-· in Figure 2a predominately arises from dissociation of nascent QH·.

As must be the case, the same temporal evolution is observed at 448 nm as at 416 nm. At pH 6.7 and $\Delta t = 5$ μs in trace b, the QH· signal has become predominately Q^-·. At pH 2.3 in trace c, only QH· is present at $\Delta t = 5$ μs, despite our high relative sensitivity to Q^-·. The generally poorer signal to noise ratio in

(9) For example, see: Champion, P. M.; Albrecht, A. C. *Chem. Phys. Lett.* **1981**, *82*, 410–413 and references contained therein.

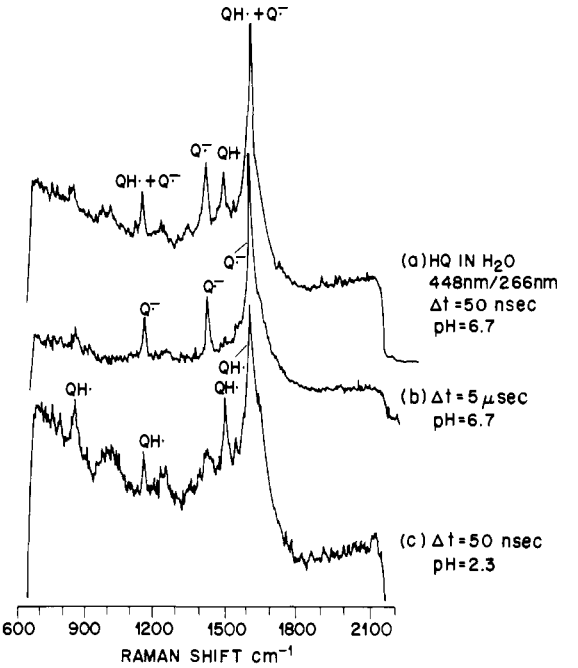

Figure 2. Similar to Figure 1, with a 448-nm probe laser ($\simeq$0.2 mJ/pulse). These spectra are an average of 3000 pulse pairs.

Figure 2 reflects weaker 448-nm resonance Raman in both species.

In the resonance Raman spectra of both Q^-· and QH·, the fluorescence background is very low. The excited-state lifetimes must be short, probably picoseconds or less, with nonradiative processes having a quantum yield of near unity. At our 416-nm flux of $\sim 3 \times 10^{17}$ photons/(cm^2·pulse), a semiquinone radical is sequentially excited several times by each 10-ns 416-nm pulse. If there were an appreciable yield of excited-state interconversion chemistry, for example, QH*· $\rightarrow$ Q^-· + H^+, then the spectra would show both QH· and Q^-· in proportions dependent upon 416-nm power. This effect is not observed; we conclude that both QH· and Q^-· have negligible interconversion quantum yields under our conditions. This result simplifies use of the transient Raman technique in observing QH· and Q^-·.

D_2O Solvent. A principal advantage of the transient Raman approach to fast kinetics is an enhanced sensitivity to structure, with the accompanying ability to detect isotopic substitution. For example, we have observed deuteration shifts in the spectra of singly and (apparently) doubly protonated triplet quinoxaline;[5a,10] such shifts are typically not observed in transient electronic absorption spectra. Since these quinone species are expected to be strongly solvated and QH· directly incorporates a proton, we studied these processes in D_2O.

As described in paper 1, photolysis of Q in H_2O produces variously triplet $Q(T_1)$, Q^-·, and QH·, as a function of Δt and pH. Within our resolution, the kinetic processes are the same, and the Q^-· and $Q(T_1)$ spectra are unchanged in D_2O. The QH· peak at 1619 cm^{-1} does show a 4 ± 3 cm^{-1} shift to lower frequency, just resolvable within our present resolution. The intensity ratio of the two strongest peaks [I(1619 cm^{-1})/I(1515 cm^{-1}) in QH·] also decreases in QD·.

Traces a and b of Figure 3 compare the 416-nm Raman spectra observed at Δt = 30 ns following 266-nm excitation of Q in H_2O and D_2O. As described in paper 1, the initial semiquinone Raman intensity increases as the square of the 266-nm power, indicating that H_2O (D_2O) is predominately oxidized by a two-photon process at these power levels ($\sim 3 \times 10^{18}$ photons/(cm^2·pulse)). Fitting the observed spectra at pH 7 indicates that the initial ratio [QH·]/[Q^-·] produced by two-photon oxidation is about 2. In Figure 3 at Δt = 30 ns and pH $\sim$2.4, the initial Q^-· fraction has been protonated to form QH· (QD·). Traces a and b also show a strong line at 1552 cm^{-1}, assigned to $Q(T_1)$. This line increases

(10) Beck, S. M.; Brus, L. E. *J. Am. Chem. Soc.* **1981**, *103*, 2495–2496.

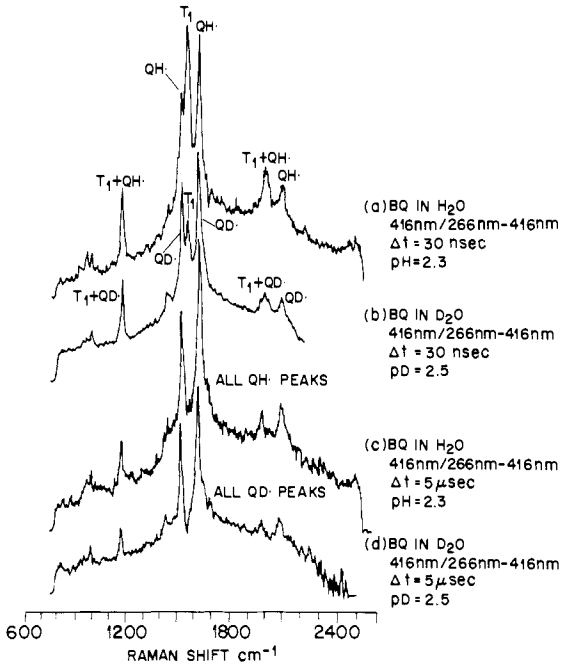

Figure 3. Raman difference spectra of aqueous benzoquinone (10^{-2} M). The spectrum from just the 416-nm laser is subtracted from the spectrum obtained with both 266-nm pump and 416-nm probe lasers. Traces a and c in H_2O, and b and d in D_2O. T_1 refers to the vibrationally relaxed lowest benzoquinone triplet.

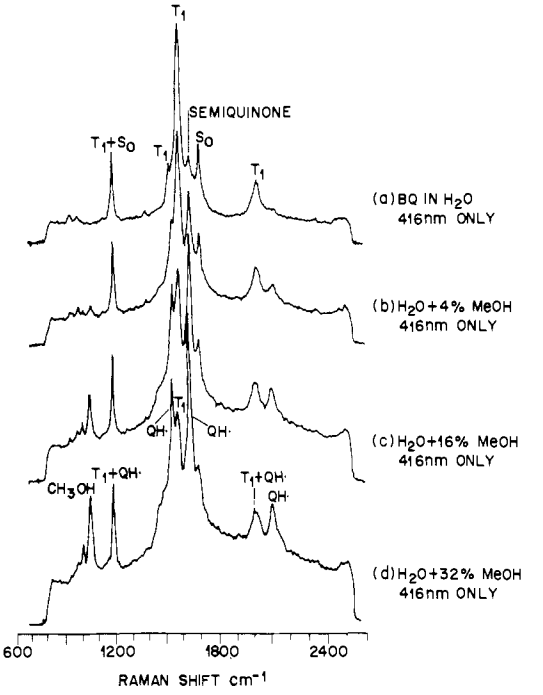

Figure 4. Raman difference spectra of aqueous benzoquinone (10^{-2} M) with increasing amounts of methanol. Each 416-nm pulse (FWHM $\simeq$ 10 ns) creates transient species and takes their Raman spectra. These spectra are an average of 600 pulses ($\simeq$1 mJ/pulse). S_0 refers to ground-electronic-state benzoquinone.

as the first power of the 266-nm intensity.[1] In both D_2O and H_2O, $Q(T_1)$ decays with $\tau \simeq 200 \pm 60$ ns.[11]

A fundamental problem in Q (but not QH_2) 416-nm Raman experiments is that the 416-nm "probe" beam also creates transient species via direct excitation of ground state Q.[1] In order to observe the time evolution of species created by the 266-nm pulse, we must eliminate the effect of excitation by the probe beam from the data. In Figure 3, we actually plot difference spectra between the 266-nm pump/416-nm probe data, and the data for 416-nm excitation alone, as a function of Δt. Due to a difference in competitive absorption of the 416-nm light in the two situations, this procedure tends to oversubtract the contribution of direct 416-nm excitation. In our present case, where the optical density at 416 nm following 266-nm excitation and the Q concentration are low, this oversubtraction is not significant.

Mixed H_2O–CH_3OH Solvents. As shown in paper 1 and Figure 4a, direct 416-nm excitation of aqueous Q produces predominantly $Q(T_1)$, and apparently a small amount of semiquinone radical, within the 10-ns width of the 416-nm pulse. The previously discussed pump–probe experiments show no concomitant increase in the semiquinone signals as $Q(T_1)$ decays, so it appears that any oxidation of H_2O yielding semiquinone radicals occurs during relaxation into the vibrationally equilibrated T_1 species. In agreement with this observation, $Q(T_1)$ redox-potential estimates suggest the relaxed triplet is not sufficiently energetic to oxidize H_2O.[1]

Addition of 1% CH_3OH decreases the 200-ns $Q(T_1)$ lifetime to $\simeq$30 ns, with a concomitant increase in the QH· signal, in experiments with both 266-nm pump and 416-nm probe beams. It is well-known that H-atom abstraction occurs more easily in alcohols than in H_2O; relaxed $Q(T_1)$ apparently abstracts H atoms from CH_3OH at a rate less than or equal to 6×10^7 M^{-1} s^{-1} in these mixed solvents.[12]

Figure 4 shows the effect of added CH_3OH in experiments where one 416-nm pulse acts as both pump and probe. The small peak of trace a in pure H_2O, tentatively assigned to semiquinone in paper 1, grows in trace b when 4% MeOH is added. In traces c and d, the initial semiquinone signal, which is $\geq$80% QH· here, grows further with a decrease in the $Q(T_1)$ signal. The increase of this small peak with added MeOH is evidence that assignment of this peak to semiquinone in H_2O solvent is correct. Nevertheless, we have not disproven the possibility that, in H_2O solvent, this peak is part of the $Q(T_1)$ spectrum. Previous studies have reported permanent oxidation products following low-flux irradiation of Q in H_2O.[13]

Discussion

Electronic and Vibrational Spectroscopy. The strong electronic transitions near 416 nm in Q^{-}·, QH·, and $Q(T_1, n-\pi^*)$ are all of similar shape, position, and intensity.[14] In Q^{-}·, this transition is assigned as a $\pi-\pi^*$ type of symmetry $^2B_{3g} \rightarrow {}^2B_{1u}$ polarized along the O atom to O-atom axis, with an experimental $f = 0.06$.[15] In a simple approximation, all three species have nine π electrons, one more than ground electronic state Q. At this level, we are dealing with the same $\pi-\pi^*$ transition of the same nine-π-electron quinone chromophore in each species. This is the basic reason the resonance Raman spectra are similar.

In S_0 Q (D_{2h} symmetry), there are two a_g normal modes of principally double-bond character. One is the symmetric stretch of the localized C=C ring bonds, and the second is the symmetric combination of the two C=O stretches. In S_0 Q, these modes are accidentally degenerate near 1650 cm^{-1} and undergo varying Fermi resonance as a function of environment.[16]

In Q^{-}·, the strong resonance Raman bands are polarized,[7] implying they represent a_g modes in this presumably D_{2h} species. Tripathi reasonably assigns the strong 1622-cm^{-1} line as principally C=C symmetric stretch (ν_{8a} in his notation).[7] In QH·, this same

(11) As discussed in ref 5, our precision in determination of temporal rates is low, certainly lower than attainable in transient absorption studies. For example, we cannot distinguish exponential decay from second-order decay. The quoted numbers are e^{-1} decay times.

(12) Note that we have not proven that all of the quenching of $Q(T_1)$ by CH_3OH leads to reaction.

(13) Kurein, K. C.; Robins, P. A. *J. Chem. Soc. B* **1970**, 855–859.

(14) There is a ~20-nm shift between Q^{-}· and QH· in ref 8, and there may be a shift of similar magnitude in the $Q(T_1)$ absorption spectrum.

(15) (a) Fukuzumi, S.; Ono, Y.; Keii, T. *Bull. Chem. Soc. Jpn.* **1973**, *46*, 3353–3355, Table 2. (b) Harada, Y. *Mol. Phys.* **1964**, *8*, 273–277. See also ref 7.

(16) Charney, E.; Becker, E. D. *J. Chem. Phys.* **1963**, *42*, 910–915. Dunn, T. M.; Francis, A. H. *J. Mol.* **1974**, *50*, 1–8.

strong line appears at 1619 cm^{-1}. Tripathi assigns the 1438-cm^{-1} line in $Q^{-}\cdot$ to be the symmetric C⁻⁻O stretch, and the 1163-cm^{-1} line to be an in-plane CH wag. We see this last line is common to $Q(T_1)$, $QH\cdot$, and $Q^{-}\cdot$. The notation C⁻⁻O implies a partial carbonyl double bond.

In $QH\cdot$, the principal change in the resonance Raman spectrum is appearance of a strong line at 1515 cm^{-1}. Physically, in $QH\cdot$, the two carbonyls have become inequivalent; both C–OH and C⁻⁻O modes may appear in the spectra. The C⁻⁻O bond in $QH\cdot$ probably has more double-bond character and lies at higher frequency than the C⁻⁻O bonds in $Q^{-}\cdot$. It is likely that this 1515-cm^{-1} line in $QH\cdot$ is the C⁻⁻O motion at the opposite end from the protonation. In agreement with this assignment, there is no detectable isotopic shift in $QD\cdot$.

$Q(T_1)$ has one strong line at 1552 cm^{-1}. It is not yet clear whether this line is a carbonyl or ring-stretch motion. Further discussion of ring-stretch and partial-carbonyl modes may be found in a recent paper on phenoxy radical resonance Raman spectra.[17]

Hydrogen Abstraction vs. Electron Abstraction. Our ability to distinguish $Q^{-}\cdot$ from $QH\cdot$ on the 10^{-8}-s time scale enables us, in favorable cases, to observe the primary photooxidation and photolysis processes. For example, Figure 4 demonstrates that, within our sensitivity, relaxed $Q(T_1)$ predominately ($\geq$80%) abstracts hydrogen atoms from CH_3OH. The 266-nm photolysis of QH_2 in H_2O also predominately yields $QH\cdot$. The two-photon photooxidation of H_2O by Q at 266 nm yields the initial ratio $[QH\cdot]/[Q^{-}\cdot] \simeq 2$.[18] The one-photon process is so weak that we are not able to fit the initial Raman spectra.

The question of electron vs. hydrogen atom abstraction has been of considerable interest for benzoquinone and duroquinone. Duroquinone apparently has a solvation-dependent T_1 state of mixed π–π^* and n–π^* character.[3] In ethanol, Amouyal and Bensasson[3] and Kemp and Porter[2] report hydrogen atom abstraction as the primary T_1 reaction. However, Scheerer and Grätzel[4] report electron abstraction from ethanol in mixed H_2O–ethanol solvent. In the case of benzoquinone, Noda et al. report electron abstraction as the primary T_1 process with ethanol.[19] We observe a predominance of hydrogen abstraction, first from CH_3OH, and second in the two-photon oxidation process in H_2O and D_2O.

Bridge and Porter originally discovered the strong tendency of quinone triplets to abstract hydrogen atoms.[20] A quinone n–π^* triplet has a localized oxidation site, a vacant n orbital, that is kinetically favorable for oxidation processes. Recent theoretical and experimental studies on isolated benzoquinone triplets have demonstrated a subtle aspect of this localization. A simple molecular orbital picture of the n–π^* triplet would suggest that the positive hole created by electron promotion is equally divided between the two oxygens. In fact, numerical calculations show that the hole is fully localized on one oxygen as in the valence bond model.[21] This is not a semantical distinction; the readjustment and polarization of the unpromoted electrons are different in the two cases. This phenomenon is experimentally reflected as an "accidental" degeneracy of the two expected n–π^* triplets.[22] Such a fully localized positive "hole" appears especially favorable in the kinetics of hydrogen atom abstraction.

Biological Applications. Quinones are widespread in nature and serve important roles as electron carriers in photosynthesis and in respiratory processes. For example, the primary electron acceptor in photosynthetic bacteria is a ubiquinone apparently perturbed by a nearby Fe atom. The kinetics of isolated reaction centers have been studied by monitoring the 450-nm transient absorption of the ubisemiquinone radical formed by electron transfer.[23,24]

The existence of strong resonance Raman signals, and the absence of significant excited-state chemistry in both $Q^{-}\cdot$ and $QH\cdot$, suggests that transient Raman kinetic studies might be made of quinones as they perform their natural functions. The transient absorption spectra of ubisemiquinone radicals in homogeneous solution are similar in strength and shape to those of *p*-benzoquinone,[8] and we expect their Raman spectra to be similar. Raman spectra observed at $\lambda \leq 500$ nm should be free of biological sample fluorescene, which occurs principally at longer wavelengths.

It is noteworthy that the biological function and the resonance Raman chromophore both (by chance) involve the quinone ring π electons. This suggests that the resonance Raman spectra will be especially sensitive to biological redox processes in varying environments. The enhanced ability of Raman data to specify structure, and to resolve isotopic substitution, suggests such kinetic studies would be informative.

Conclusions

(1) The resonance Raman spectra of $Q(T_1)$, $QH\cdot$, and $Q^{-}\cdot$ have been observed, and the major lines are assigned, confirming and extending a previous assignment for $Q^{-}\cdot$. The spectrum of $QD\cdot$ is distinguishable from that of $QH\cdot$.

(2) The 266-nm photolysis of aqueous QH_2 yields predominately $QH\cdot$, without intermediates, at 10^{-8} s. $Q(T_1)$ reacts with CH_3OH to yield predominately $QH\cdot$. Two-photon 266-nm photolysis of aqueous benzoquinone yields the initial ratio $[QH\cdot]/[Q^{-}\cdot] \simeq 2$, under the assumption that both species have the same resonance Raman cross section

(3) An acid–base equilibrium between $QH\cdot$ and $Q^{-}\cdot$ is consistent with the previously reported $pK_a = 4.1$. The time-resolved spectra show unimolecular dissociation of $QH\cdot$ at neutral pH and near-diffusion-limited protonation of $Q^{-}\cdot$ at low pH.

(4) Single-photon 416-nm excitation of aqueous Q produces predominately $Q(T_1)$ with an additional small yield of water photooxidation, apparently during relaxation to the equilibrated T_1 state. The T_1 lifetime is 200 ± 60 ns in both D_2O and H_2O. The T_1 transient absorption substantially overlaps the semiquinone absorptions.

Note Added in Proof. Dr. R. V. Bensasson has kindly brought to our attention an article (Ronfard-Haret, J. C.; Bensasson, R. V.; Amouyal, E. *J. Chem. Soc., Faraday Trans. 1* **1980**, *76*, 2432–2436) in which the transient absorption of aqueous $Q(T_1)$ was detected. These authors have also concluded that $Q(T_1)$ oxidizes H_2O to yield $QH\cdot$.

Registry No. Q, 106-51-4; QH_2, 123-31-9; $QH\cdot$, 3225-30-7; $Q^{-}\cdot$, 3225-29-4.

(17) Beck, S. M.; Brus, L. E. *J. Chem. Phys.* **1982**, *76*, 4700–4704.
(18) The very short first excited-singlet-state lifetimes and the high quantum yield for triplet formation suggest, but do not prove, that the second photon is absorbed by triplet benzoquinone.
(19) Noda, S.; Doba, T. Mizuta, T.; Miura, M.; Yoshida, Y. *J. Chem. Soc., Perkin Trans. 2* **1980**, 61–64.
(20) Bridge, N. K.; Porter, G. *Proc. R. Soc. London, Ser. A* **1958**, *244*, 259–276.
(21) Jonkman, H. T.; van der Velde, G. A.; Nieuwpoort, W. C. "Quantum Chemistry—State of the Art"; Oxford Press: New York, 1974.
(22) Goodman, J.; Brus, L. E. *J. Chem. Phys.* **1978**, *69*, 1604–1612.
(23) Wraight, C. A. *Biochim. Biophys. Acta* **1979**, *548*, 309–327.
(24) Vermeglio, A.; Clayton, R. K. *Biochim. Biophys. Acta.* **1977**, *461*, 159–165.